

## Supporting information

# Exploring Paclitaxel-Albumin-Loaded Neutrophil-Like Cells via Microfluidic-Based Mechanical Deformation for Enhanced Cargo Delivery in Glioblastoma Therapy

Daidi Zhou<sup>a</sup>, Xinghua Gao<sup>a\*</sup> <sup>ζ</sup>, Zhiyu Mao<sup>a</sup>, Xiaoling Yang<sup>a</sup>, Jingyun Ma<sup>c</sup>, Ekaterina Andreevna Vorotelyak<sup>f c g</sup>, Guohui Hu<sup>b</sup>, Fengping Zhu<sup>d h \*</sup>, and Jinbo Wu<sup>a c \*</sup>

<sup>a</sup> Materials Genome Institute, Shanghai University, Shanghai 200444, China.

<sup>b</sup> Shanghai Institute of Applied Mathematics and Mechanics, School of Mechanics and Engineering Science, Shanghai University, Shanghai 200072, China.

<sup>c</sup> Faculty of Materials Science, Shenzhen MSU-BIT University, Shenzhen 518172, China.

<sup>d</sup> Department of Neurosurgery, Huashan Hospital, Shanghai Medical College, Fudan University, Shanghai, China.

<sup>e</sup> Ningbo Institute of Innovation for Combined Medicine and Engineering, The Affiliated Lihuili Hospital of Ningbo University, Ningbo, Zhejiang, 315040, China.

<sup>f</sup> Department of Cell Biology and Histology, Biological Faculty, Lomonosov Moscow State University.

<sup>g</sup> N.K. Koltzov Institute of Developmental Biology, Russian Academy of Sciences.

<sup>h</sup> The Fourth Division Hospital of Xinjiang Production and Construction Corps, Yining, China.

<sup>ζ</sup> Co-first authors

### Corresponding Authors :

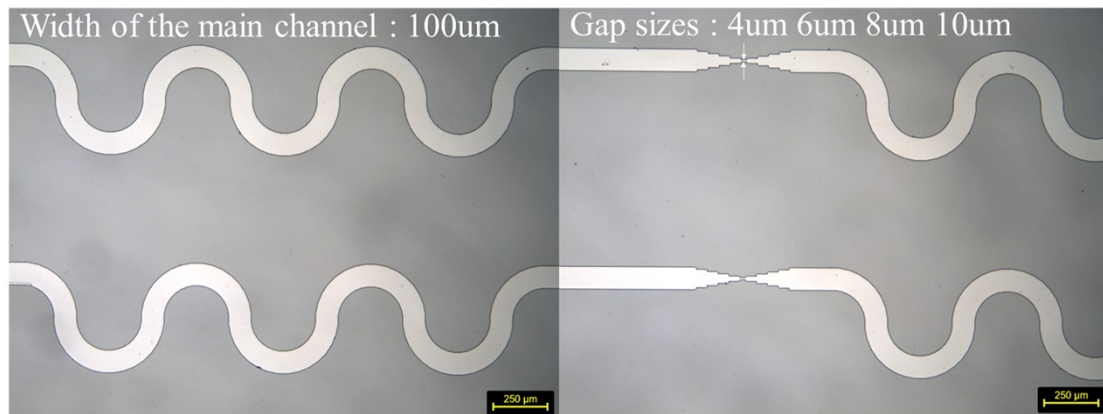
\* Prof. Xinghua Gao, gaoxinghua@t.shu.edu.cn (orcid.org/0000-0002-5244-0986);

\* Prof. Fengping Zhu, fpzhu@fudan.edu.cn;

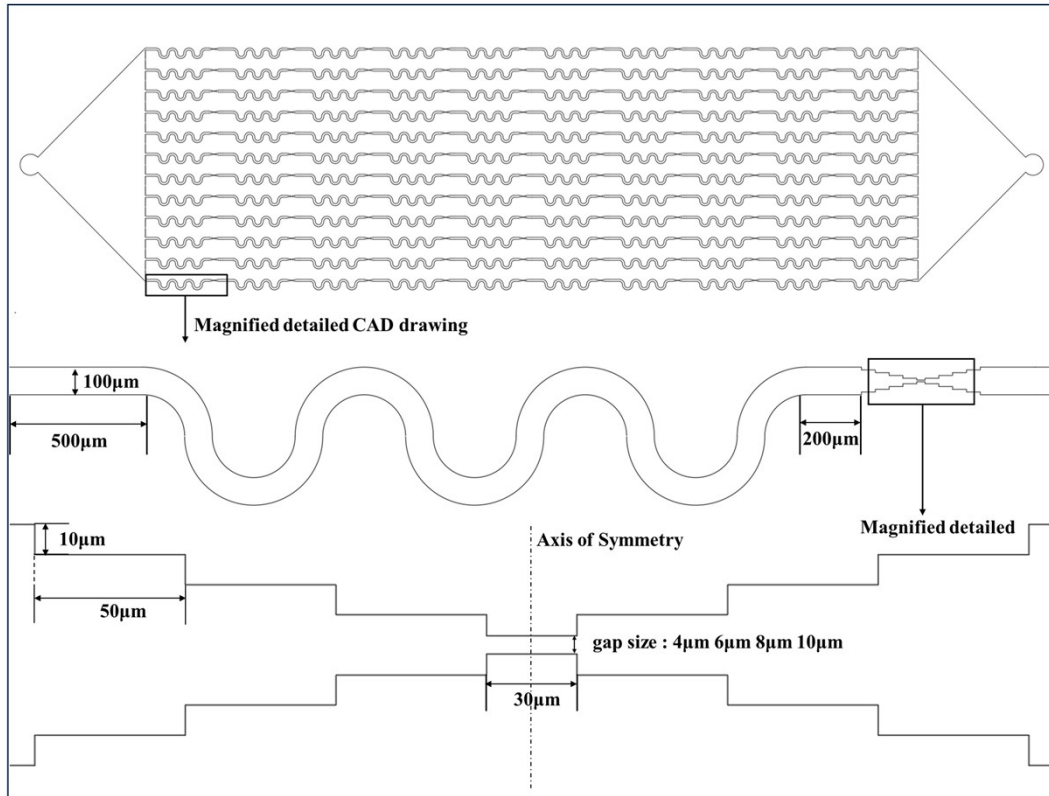
\* Prof. Jinbo Wu, jinbowu@smbu.edu.cn.

**Supplementary video 1.** Video of HL-60 cells passing through the serpentine channel in the microchannel.

**Supplementary video 2.** Video of HL-60 cells passing through the constriction gap in the microchannel.



**Supplementary Figure 1.** A micrograph showing the detailed channel structure of the microfluidic chip.



**Supplementary Figure 2.** A CAD drawing of the microfluidic chip. It should be noted that the chip design employs multiple constriction structures to improve delivery efficiency. The use of 10 constrictions is based on the consideration that if the success rate per constriction reaches 50%, then the cumulative success rate after 10 consecutive constrictions can reach 99.9%. This study did not optimize this parameter; therefore, there is room for further exploration of this parameter.

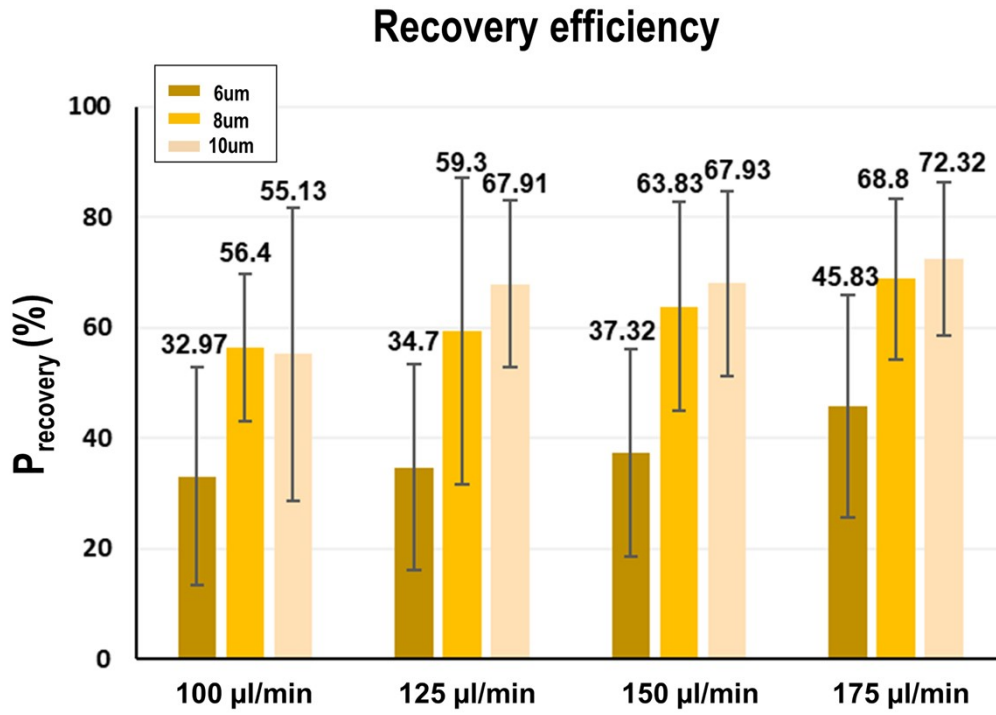
**Supplementary Table 1.** Reynolds number and wall shear stress from the main channel to the minimum constriction gap segment in the microfluidic chip.

Segment No.	Width ( $\mu\text{m}$ )	Area ( $\text{m}^2$ )	Hydraulic Diameter ( $\text{D}_h$ (m))	Average Flow Velocity ( $u$ (m/s))	Re	Wall shear stress	
						$\tau_w$ (Pa) $\mu=0.001$ Pa·s	$\tau_w$ (Pa) $\mu=0.0015$ Pa·s
1	100	$1.10 \times 10^{-9}$	$1.982 \times 10^{-5}$	0.189	3.75	103.3	154.9
2	80	$8.80 \times 10^{-10}$	$1.934 \times 10^{-5}$	0.237	4.58	129.1	193.7
3	60	$6.60 \times 10^{-10}$	$1.859 \times 10^{-5}$	0.316	5.87	172.2	258.3
4	40	$4.40 \times 10^{-10}$	$1.726 \times 10^{-5}$	0.473	8.17	258.3	387.4
5	20	$2.20 \times 10^{-10}$	$1.419 \times 10^{-5}$	0.947	13.44	516.5	774.8
6	8	$8.80 \times 10^{-11}$	$9.263 \times 10^{-6}$	2.367	21.93	1291.3	1937.0

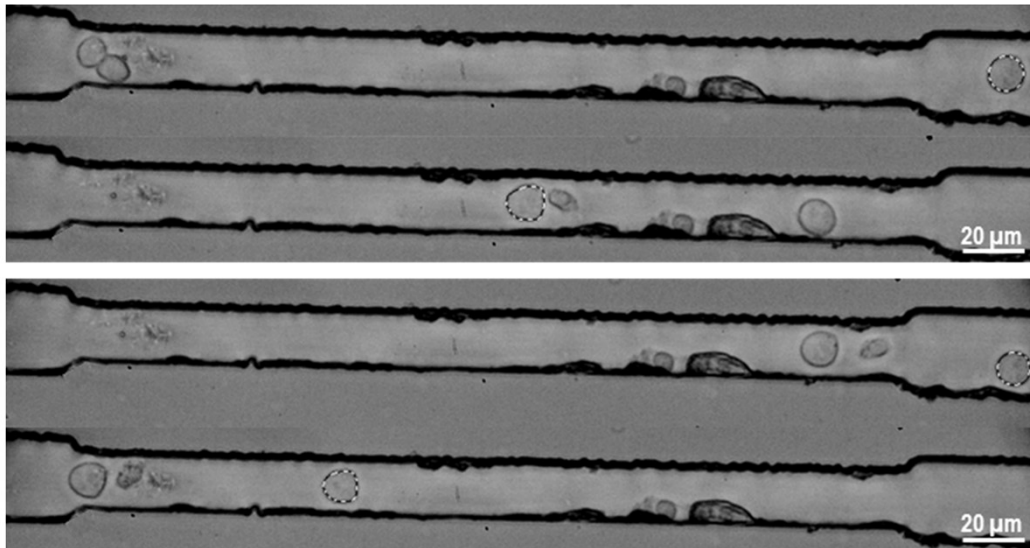
The overall inlet flow rate was 150  $\mu\text{L}/\text{min}$ . Dynamic viscosity was estimated based on the water  $\mu=0.001$  Pa · s. The dynamic viscosity was estimated based on the medium containing cells and FITC-Dextran  $\mu=0.0015$  Pa · s. Studies have indicated that the critical tensile stress for chinese hamster ovary (CHO) cells and human embryonic kidney (HEK) cells is around 500 Pa [40]. Based on calculations, the wall shear stress experienced by cells before entering the minimum constriction gap is approximately 500 Pa, while the wall shear stress provided within the minimum constriction gap segment is about 2.4 times higher, approximately 1200 Pa. Therefore, effective cell deformation is primarily induced within the minimum constriction gap segment.

**Supplementary Table 2.** Dean number of the main channel at different flow rates.

Total flow rate ( $\mu\text{L}/\text{min}$ )	Flow rate per single channel ( $\mu\text{L}/\text{min}$ )	Re	Dean Number (De)	Wall shear stress (Pa)
100	8.33	2.50	0.56	68.9
125	10.42	3.13	0.69	86.1
150	12.50	3.75	0.83	103.3
175	14.58	4.38	0.97	120.5



**Supplementary Figure 3.** Histogram of cell recovery rate ( $P_{\text{recovery}}$ ). Approximately  $10^6$  HL-60 cells were passed through the microfluidic chip with different gap sizes and flow rates.  $N = 3$ .



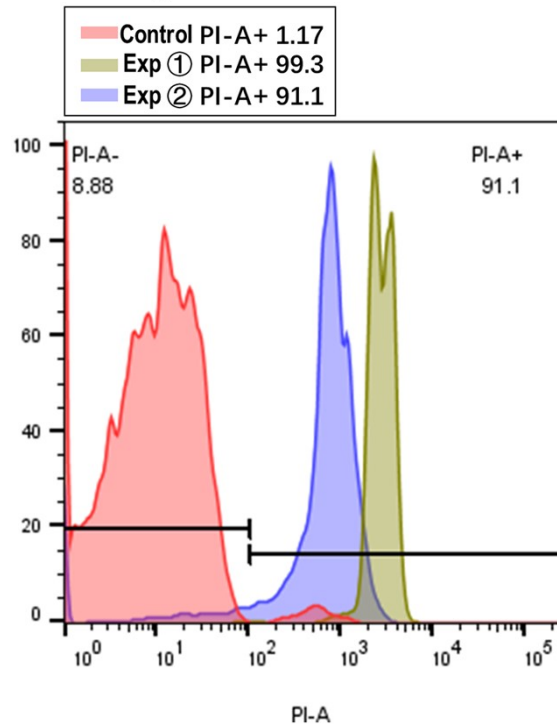
**Supplementary Figure 4.** Image series of HL-60 cell deformation. Observed chip dimensions: height 20  $\mu\text{m}$ , widths 30  $\mu\text{m}$  and 20  $\mu\text{m}$ . We calculated the deformation degree (D) of HL-60 cells using the formula from reference [41]:

$$D = 1 - c = 1 - \frac{2\sqrt{\pi \cdot A}}{l}$$

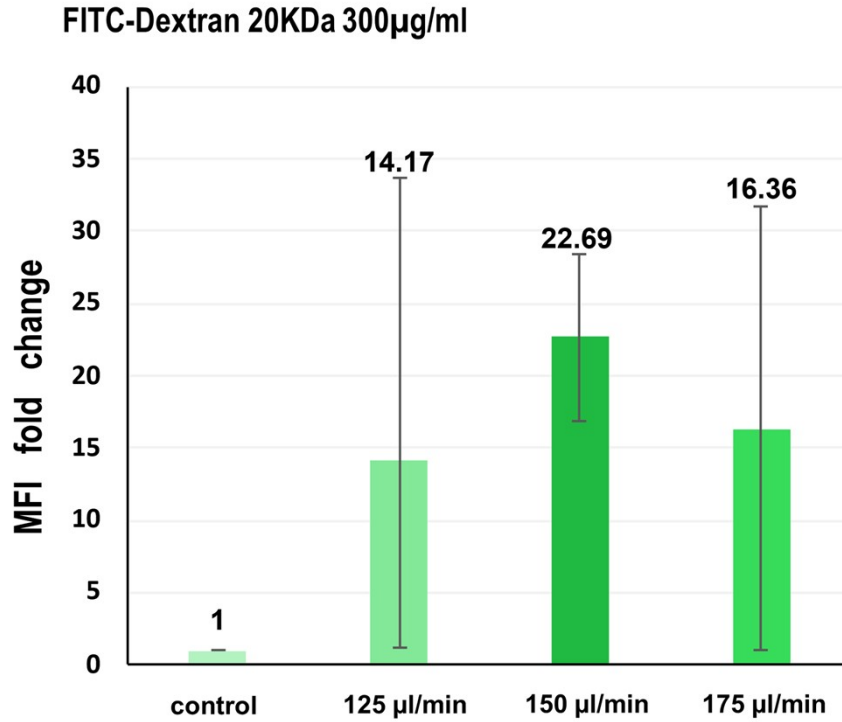
where  $c$  is the circularity of the cell upon deformation,  $A$  is the deformed cell area, and  $l$  is the deformed cell perimeter. The calculated deformation degrees for HL-60 cells were 0.06645 and 0.0618, which fall within the range reported in existing studies [42]. Cell deformation degree is closely related to cellular stiffness.

Under the same experimental conditions, a higher deformation degree indicates softer cells with lower stiffness, making them more susceptible to effective mechanical deformation under applied force. This results in the formation of transient pores in the cell membrane, thereby facilitating passive diffusion of cargo into the cells [42]. Existing studies [37] show that the deformation degree of HL-60 cells ranges approximately between 0.04 and 0.06. Compared to other cell lines—such as Hela K cells (~0.01–0.04), PRE-1 cells (~0.01–0.04), U2OS cells (~0.02–0.05), and BJ cells (~0.01–0.04)—HL-60 cells are relatively more prone to mechanical deformation.

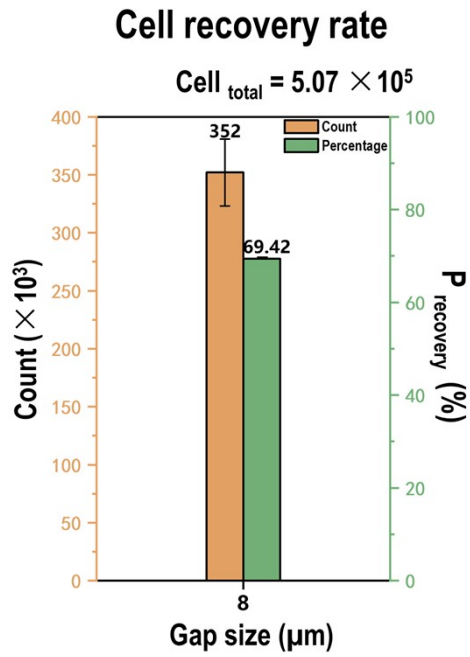
## Inducing the death of HL-60 cells



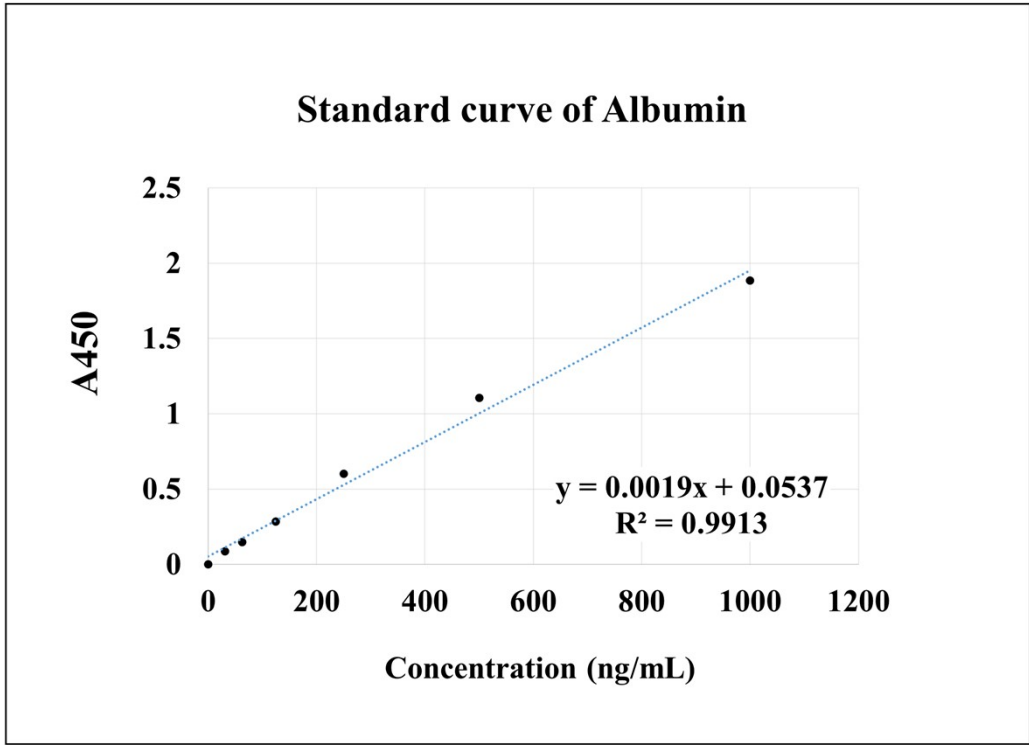
**Supplementary Figure 5.** Representative plot of PI positivity threshold. The PI-positive threshold was determined by inducing HL-60 cell death and using the standard PI staining method. Control group: Untreated cells. Experimental group ①: The HL-60 cell suspension was centrifuged, the supernatant was removed, and the cells were resuspended in PBS. The suspension was then placed in a 70 °C water bath for 10 minutes, during which the tube was gently inverted once to prevent cell sedimentation. Subsequently, the cells were cooled at room temperature for 5 minutes. Experimental group ②: A 70% ethanol solution was prepared using absolute ethanol and PBS, and pre-cooled to -20 °C. The HL-60 cell suspension was centrifuged, the supernatant was discarded, and the cells were resuspended in pre-cooled PBS. After another centrifugation and removal of the supernatant, pre-cooled 70% ethanol was added. The cells were then fixed at 4 °C for 30 minutes.



**Supplementary Figure 6.** Histogram showing fold changes in the mean fluorescence intensity (MFI). HL-60 cells were passed through the microfluidic chip with different flow rates at the gap size of 8 µm. The delivered cargo was FITC-Dex (20kDa) at concentration 300 µg/ml. N = 3.



**Supplementary Figure 7.** Histogram of the number of recovered cells and cell recovery rate (P<sub>recovery</sub>) of neutrophil-like cells. Approximately  $5.07 \times 10^6$  neutrophil-like cells were passed through the microchip with a gap size of  $8 \mu\text{m}$ . The flow rate was  $150 \mu\text{L}/\text{min}$ .



**Supplementary Figure 8.** Standard curve of the ELISA for albumin.